LASER & PHOTONICS REVIEWS
www.lpr-journal.org

Remote Preparation of Optical Cat States Based on Gaussian Entanglement

Dongmei Han, Fengxiao Sun, Na Wang, Yu Xiang, Meihong Wang, Mingsheng Tian, Qiongyi He, and Xiaolong Su**

Remote state preparation enables one to prepare and manipulate quantum state non-locally. As an essential quantum resource, optical cat state is usually prepared locally by subtracting photons from a squeezed vacuum state. For remote quantum information processing, it is essential to prepare and manipulate optical cat states remotely based on Gaussian entanglement, which remains a challenge. Here, experimental preparation of optical cat states based on a remotely distributed two-mode Gaussian entangled state in a lossy channel is presented. By performing photon subtraction and homodyne projective measurement at Alice's station, an optical cat state is prepared remotely at Bob's station. Furthermore, the prepared cat state is rotated by changing Alice's measurement basis of homodyne detection, which demonstrates the remote manipulation of it. By distributing two modes of the two-mode Gaussian entangled state in lossy channels, it is demonstrated that the remotely prepared cat state can tolerate much more loss in Alice's channel than that in Bob's channel. It is also shown that cat states with amplitudes larger than 2 can be prepared by increasing the squeezing level and subtracting photon numbers. The results make a crucial step toward remote hybrid quantum information processing involving discrete- and continuous-variable techniques.

1. Introduction

With the development of quantum communication and quantum network, it becomes possible for a user without the ability of preparing quantum state to obtain quantum resources. Generally, there are several options to achieve this goal, such as direct state transmission, remote state preparation (RSP),[1,2] and quantum teleportation,[3] respectively. RSP enables one to create and control a quantum state remotely based on shared entanglement. Compared with the direct state transmission, where a prepared quantum state is directly transmitted to the user through a lossy channel, RSP offers remote control of quantum state and intrinsic security.[4,5] Compared with quantum teleportation, RSP does not need joint measurement, requires less classical communication,[6] and offers the ability to manipulate quantum state remotely.

Schrödinger cat states play important roles in both fundamental physics and quantum information, such as exploring the boundary between quantum and classical physics,[7–9] quantum computation,[10–13] quantum communication,[14–17] and quantum metrology.[18–20] Free-propagating optical cat states have attracted much attention attributed to their weak interaction with the environment, which is beneficial to quantum information processing. Up to now, most of the reported optical cat states are prepared locally by subtracting photons from squeezed vacuum states,[21–27] which combines the discrete-variable technology and continuous-variable resource.[28] However, this method sets a barrier for the users since it requires the ability of creating squeezed states and performing a non-Gaussian operation.

Recently, RSP has been applied to prepare non-Gaussian states,[29–31] which demonstrate the connection between remotely prepared Wigner negativity and quantum steering. As for a special kind of non-Gaussian states, cat states have also been prepared by RSP based on a two-photon Fock state,[32] a two-photon N00N state,[33] hybrid discrete- and continuous-variable entanglement[34,35] and optomagnetic entanglement.[36] In most previous experiments,[33,34] the RSP of cat states demonstrates the generation of a non-Gaussian state from a non-Gaussian entangled resource. Compared with preparing the non-Gaussian

D. Han, N. Wang, M. Wang, X. Su
State Key Laboratory of Quantum Optics and Quantum Optics Devices
Institute of Opto-Electronics
Shanxi University
Taiyuan 030006, China
E-mail: suxl@sxu.edu.cn

F. Sun, Y. Xiang, M. Tian, Q. He
State Key Laboratory for Mesoscopic Physics
School of Physics
Frontiers Science Center for Nano-optoelectronics
Peking University
Beijing 100871, China
E-mail: qiongyihe@pku.edu.cn

Y. Xiang, M. Wang, Q. He, X. Su
Collaborative Innovation Center of Extreme Optics
Shanxi University
Taiyuan, Shanxi 030006, China

Q. He
Peking University Yangtze Delta Institute of Optoelectronics
Nantong, Jiangsu 226010, China

The ORCID identification number(s) for the author(s) of this article can be found under https://doi.org/10.1002/lpor.202300103

DOI: 10.1002/lpor.202300103

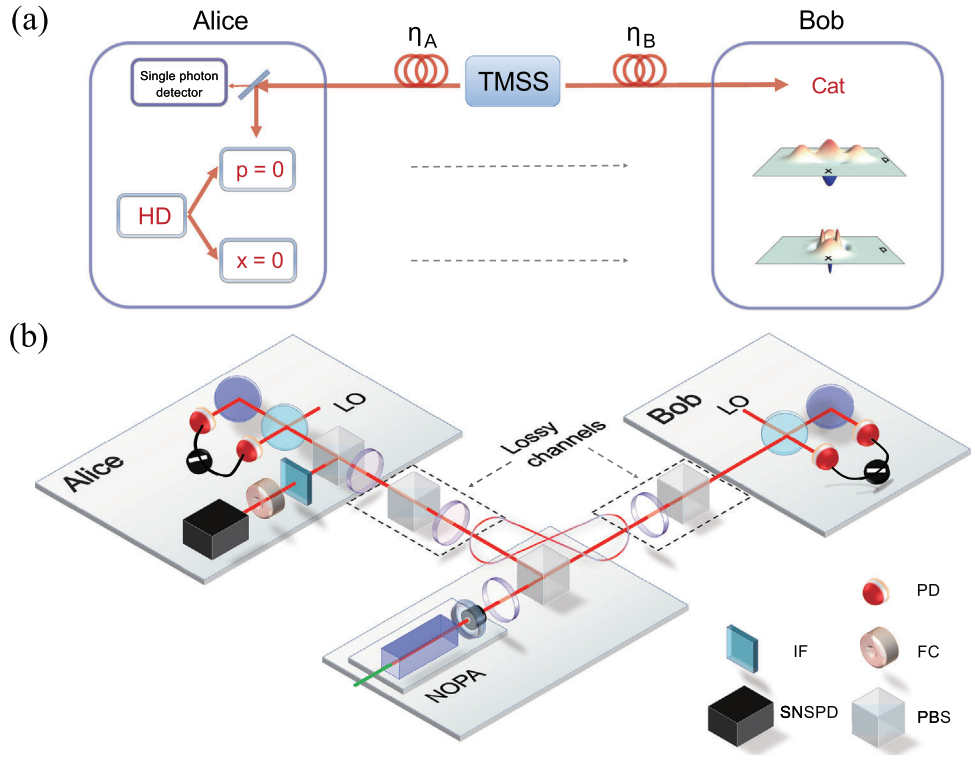

Figure 1. Schematic and experimental setup. a) The principle of the experiment. Alice implements photon subtraction by using a single-photon detector and homodyne projective measurement on one mode of the TMSS. A cat state or rotated cat state for 90 degrees is created at Bob's station conditioned on the measurement results of $p_A = 0$ or $x_A = 0$. b) Experimental setup. Bob's lossy channel is simulated by the combination of a half-wave plate (HWP) and a polarization beam splitter (PBS). TMSS, two-mode squeezed state; HD, homodyne detector; NOPA, non-degenerate optical parametric amplifier; PD, photodiode; IF, interference filter; FC, filter cavity; SNSPD, superconducting nanowire single photon detector; LO, local oscillator.

entangled resource, such as the N00N state and hybrid entangled state, Gaussian entangled states can be prepared deterministically and present scalability.[37–42] However, it still remains a challenge to experimentally prepare and manipulate optical cat states remotely based on Gaussian entanglement.

Here, we experimentally demonstrate the preparation of cat states at a distant node based on a distributed Gaussian entangled state in a lossy channel. Alice, who has the ability to perform photon subtraction, and Bob, who does not, share a two-mode squeezed state (TMSS) remotely. By implementing photon subtraction and homodyne projective measurement on Alice's state, Bob's state collapses to a cat state conditionally. An optical odd cat state with amplitude of ≈ 0.65 and fidelity of ≈ 0.67 is created at a generation rate of 1 kHz by projecting on phase quadrature at Alice's station when the transmission efficiency on Bob's mode is 0.9. Then, the cat state is rotated for 90 degrees by converting the projective measurement to amplitude quadrature at Alice's station, which demonstrates remote manipulation of the prepared state. Moreover, remote preparation of optical cat states is achieved when Alice's or Bob's state is transmitted through a lossy channel. We also show that the amplitudes of the prepared cat states can be increased by subtracting more photons from a TMSS with optimum squeezing. In principle, this scheme can remotely prepare odd or even cat states by subtracting odd or even photon numbers at Alice's station. Thus, our result provides a new method to remotely generate and manipulate optical cat states.

2. The Principle

As shown in **Figure 1**a, a TMSS of the form $|\psi_0\rangle_{AB} = \frac{1}{\cosh r}\sum_{m=0}^{\infty}\tanh^m r|m,m\rangle_{AB}$ is prepared, where r is the squeezing parameter, and then two modes of the entangled state are sent to Alice and Bob through lossy quantum channels with transmission efficiencies of η_A and η_B respectively. Alice performs photon subtraction on her state and measures the photon-subtracted state with a homodyne detector (HD). By measuring the quadrature $\hat{x}_A^\theta = (\hat{a}_A e^{-i\theta} + \hat{a}_A^\dagger e^{i\theta})/\sqrt{2}$ and projecting the output to $x_A^\theta = 0$, where $\hat{a}_A$ is the annihilation operator and θ is a general phase, an odd cat state is remotely prepared at Bob's station. Especially, $\hat{x}_A^\theta$ corresponds to the amplitude quadrature ($\hat{x}_A$) for $\theta = 0$ and the phase quadrature ($\hat{p}_A$) for $\theta = \pi/2$. And the eigenstate $|x_A^\theta\rangle_A$ with corresponding eigenvalue x_A^θ is expressed by the inner product with the photon number state $|m\rangle$

$$ {}_A\langle x_A^\theta|m\rangle_A = \frac{e^{-im\theta}}{\sqrt{2^m m!\sqrt{\pi}}} e^{-(x_A^\theta)^2/2} H_m(x_A^\theta) \tag{1}$$

where $H_m(x)$ is the Hermite polynomial.

For an arbitrary quadrature measurement $\hat{x}_A^\theta$ with the outcome chosen as $x_A^\theta = 0$, the ideal conditional state obtained at Bob's station becomes $|\varphi\rangle_B = {}_A\langle 0^\theta|\hat{a}_A|\psi_0\rangle_{AB} \propto \sum_{m=1}^{\infty}\sqrt{m/2^{m-1}(m-1)!}e^{-i(m-1)\theta}\tanh^m r H_{m-1}(0)|m\rangle_B$. Since

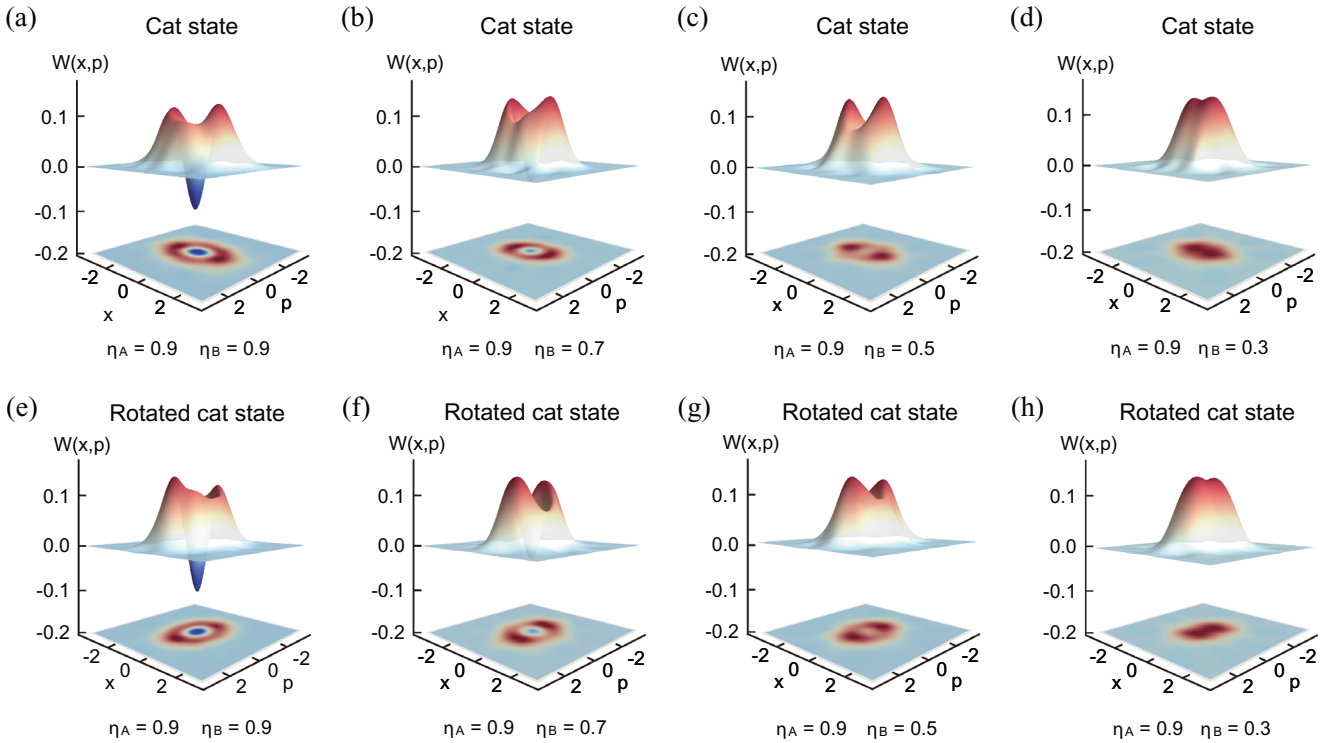

Figure 2. Reconstructed Wigner functions and corresponding contour plots of prepared states at different transmission efficiency η_B. a–d) Cat states and e–h) rotated cat states for 90 degrees at different transmission efficiencies of Bob's mode. All results in the above plot are corrected with 90% detection efficiency.

$H_{2k}(0) = (-2)^k(2k-1)!!$ and $H_{2k+1}(0) = 0$, the state can be simplified as

$$|\varphi\rangle_B \propto |r,\theta\rangle_B - |-r,\theta\rangle_B \tag{2}$$

with $|r,\theta\rangle_B \propto \sum_{m=0}^{\infty} \frac{m!!}{\sqrt{m!}} e^{-im(\theta-\pi/2)} \tanh^m r |m\rangle_B$ (see Section S1, Supporting Information for more details). Hence, if Alice measures the phase quadrature ($\hat{p}_B$), Bob's state is similar to an odd cat state $|cat\_\rangle = (|\alpha\rangle - |-\alpha\rangle)/\sqrt{2(1-e^{-2|\alpha|^2})}$ with the real number α. Ideally, the fidelity $F = \langle cat\_|\rho_B|cat\_\rangle$ between Bob's state $\rho_B = |\varphi\rangle_{BB}\langle\varphi|$ and the odd cat state $|cat\_\rangle$ reaches $\approx 99\%$ with 3 dB squeezing of the TMSS (see Section S1, Supporting Information for more details). If Alice measures the amplitude quadrature ($\hat{x}_A$), Bob's conditional state is similar to the state $(|i\alpha\rangle - |-i\alpha\rangle)/\sqrt{2(1-e^{-2|\alpha|^2})}$, which is equivalent to applying a rotation operation by 90 degrees $\hat{R}(\pi/2)$ on the odd cat state $|cat\_\rangle$. This indicates that Bob's cat state can be remotely manipulated by choosing the basis of Alice's homodyne projective measurement.

3. The Experiment

As shown in Figure 1b, when the non-degenerate optical parametric amplifier (NOPA) is working at amplification status, where the relative phase between seed beam (1080 nm) and pump beam (540 nm) is locked to 0, a TMSS with squeezing and antisqueezing levels of −3.2 and +4.2 dB is prepared when we inject 70 mW pump power into the NOPA.[43–45] (see Section S2, Supporting Information for more details). To perform photon subtraction operation, Alice uses a variable beamsplitter composed of a half-wave plate (HWP) and a polarization beam splitter (PBS) to tap around 4% of her mode toward the superconducting nanowire single-photon detector (SNSPD). An interference filter with 0.6 nm bandwidth together with a filter cavity with 400 MHz bandwidth are placed in front of the SNSPD to select the degenerate mode of the NOPA. To avoid the reflection from the front mirror of the filter cavity to the NOPA, an optical isolator is placed in front of the interference filter. An SNSPD with around 70% detection efficiency, which only influences the generation rate of the prepared state, is used to detect the subtracted photons and the clicks of it are used to trigger the storage oscilloscope for the data recording of Alice's and Bob's homodyne detectors (HDs). Our experiment is conducted in the locking-and-hold mode, where the seed beam is injected into the NOPA for the cavity locking during the locking period (≈50 ms), and it is chopped off to obtain the TMSS during the hold period (≈30 ms) (see Section S2, Supporting Information for more details).

To realize the homodyne projective measurement, the amplitude quadrature $\hat{x}_A$ or phase quadrature $\hat{p}_A$ of the photon-subtracted state is measured by Alice's homodyne detector and then post selected with a selection width of $\delta x < 0.05$ on $\hat{x}_A$ ($\hat{p}_A$). Alice and Bob record the output signals of their HDs simultaneously, and then Bob only keeps the corresponding data when Alice's quadrature values meet the selection condition. Bob performs quantum tomography to reconstruct the Wigner function $W(x,p)$ of his state.

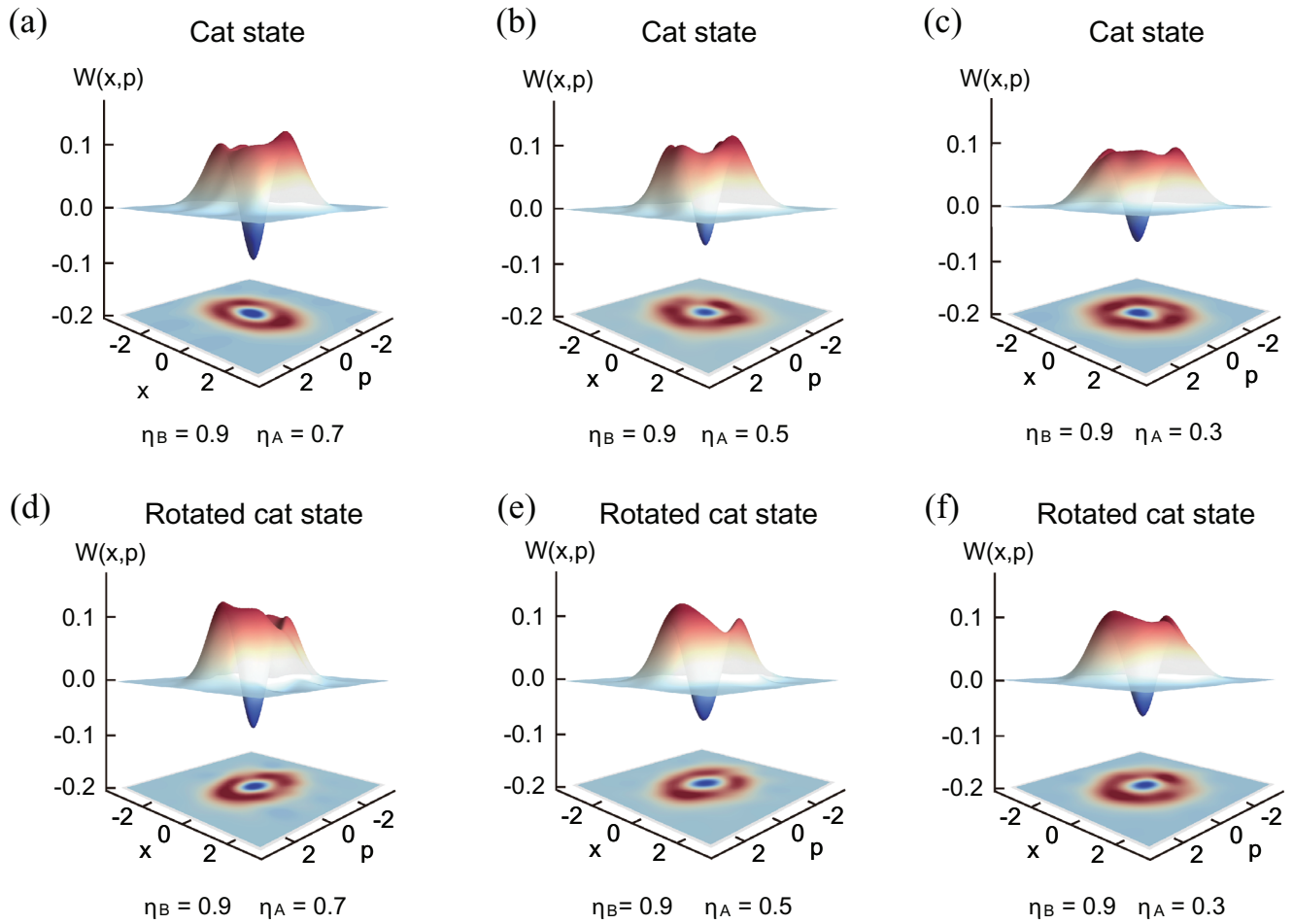

Figure 3. Reconstructed Wigner functions and corresponding contour plots of prepared states at different transmission efficiency η_A. a–c) Cat states and d–f) rotated cat states for 90 degrees at different transmission efficiencies of Alice's mode. All results in the above plot are corrected with 90% detection efficiency.

4. Results

As shown in **Figure 2**a,e, optical cat states with two directions in phase space are prepared by projecting Alice's quadrature values at $p_A = 0$ and $x_A = 0$, respectively. In principle, cat states at Bob's station could be rotated in arbitrary directions with the form of $(|e^{i\theta}\alpha\rangle - |e^{-i\theta}\alpha\rangle)/\sqrt{2(1-e^{-2|\alpha|^2})}$ by changing the homodyne projection angle θ at Alice's station (see Section S1, Supporting Information for more details), which shows remote manipulation of directions of prepared cat states in phase space. Compared with the preparation of cat states in arbitrary directions based on photon subtraction from squeezed vacuum states, which requires squeezed vacuum states squeezed in arbitrary directions, the presented scheme relaxes this requirement on the quantum resource.

An optical cat state and a rotated cat state with amplitude $|\alpha| \approx 0.65$ and the value of $W(0,0) \approx -0.10$ are obtained when transmission efficiency is $\eta_A = \eta_B = 0.9$. The fidelity of the prepared optical cat state $F = \langle cat\_|\rho_{out}|cat\_\rangle$ is quantified by calculating the overlap between an ideal cat state $|cat\_\rangle$ and the experimentally reconstructed density matrix ρ_{out}. An optical cat state and a rotated cat state with the fidelity of $F \approx 67\%$ are obtained, which is limited by the purity of the initial TMSS and loss, at the transmission efficiency of 0.9.

To present the tolerance of our scheme on channel loss, we simulate the transmission of Alice's and Bob's modes of the TMSS in lossy channels by changing the transmission efficiency in Alice's and Bob's quantum channels respectively. In the case of loss on Bob's mode, as shown in Figure 2, the negative values of $W(0,0)$ of the prepared cat state and the rotated cat state are reduced when the transmission efficiency is varied from 0.9 to 0.3, which represents the decrease of the nonclassical feature. The negative part of the Wigner function vanishes at the transmission efficiency of 0.5 and 0.3.

In the case of loss on Alice's mode, as shown in **Figure 3**, cat and rotated cat states are also obtained at Bob's station. The negative value of $W(0,0)$ of prepared states is reduced when the transmission efficiency is varied from 0.7 to 0.3, but it never disappears. Compared with the case of loss in Bob's mode (Figure 2), the loss tolerance of our scheme in Alice's mode is better than that in Bob's mode.

To quantify the characteristics of remotely prepared cat states in a lossy quantum channel, we present the value of $W(0,0)$, fidelities, and amplitudes of prepared states at different

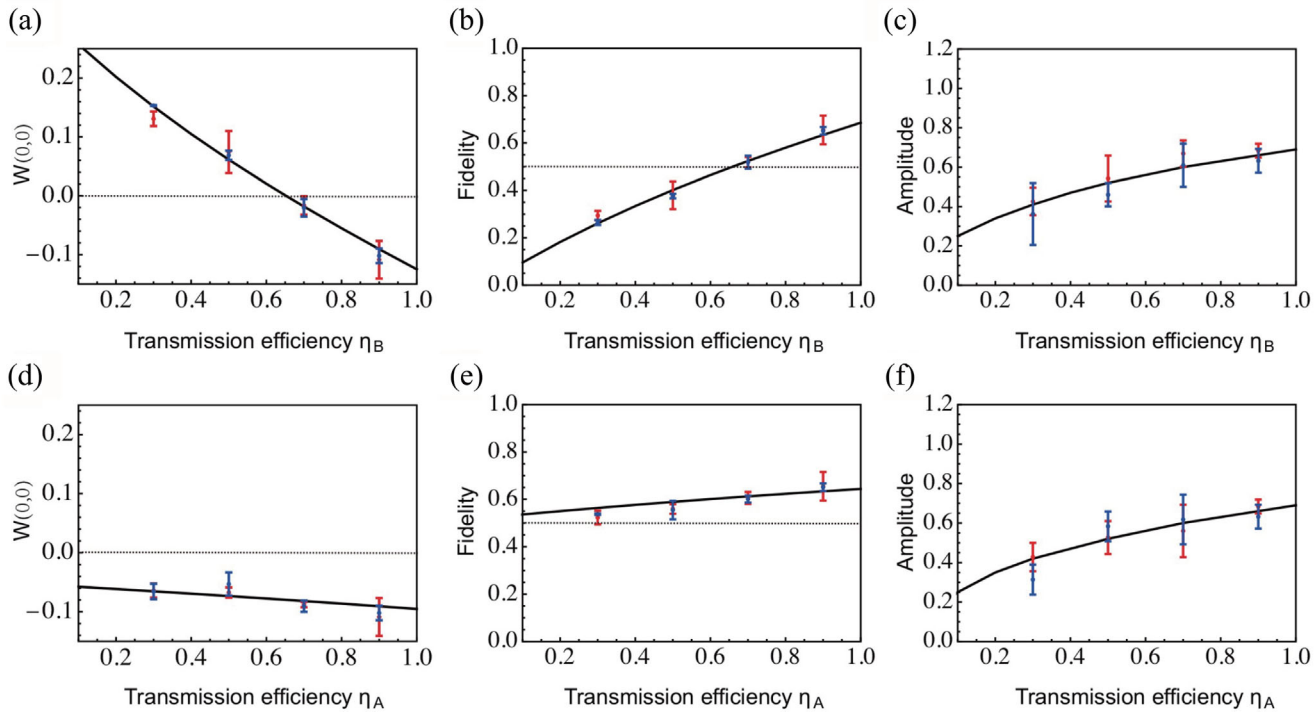

Figure 4. Evolution of remotely prepared cat states in a lossy quantum channel. a) The Wigner negativity, b) fidelity, and c) amplitude of the remotely prepared cat states as a function of the transmission efficiency of Bob's mode. d) The Wigner negativity, e) fidelity, and f) amplitude of the remotely prepared cat states as a function of the transmission efficiency of Alice's mode. The red and blue data points represent cat states and rotated cat states for 90 degrees, respectively. The error bars are obtained by the standard deviation of measurements repeated three times.

transmission efficiencies in Bob's and Alice's channels in **Figure 4**. In the case of loss on Bob's channel (Figure 4a–c), it is obvious that the fidelity and amplitude of remotely prepared cat states are reduced with the decrease in transmission efficiency. When the transmission efficiency of Bob's mode surpasses 0.64, the fidelity is larger than 50%, and negativity of the Wigner function appears, which indicates that cat states are successfully prepared remotely within the transmission distance of ≈ 9 km (considering a loss rate of 0.2 dB km^{-1} in the fiber channel).

In the case of loss on Alice's channel (Figure 4d–f), it is obvious that the negativity of the Wigner function, fidelity, and amplitude of remotely prepared cat states is reduced with the decrease of transmission efficiency. However, the fidelity of the remotely prepared cat state is always above 0.5 as long as the transmission efficiency in Alice's mode is larger than zero, which is different from that in the case of loss on Bob's channel. This demonstrates that the remotely prepared cat state can tolerate much more loss in Alice's channel than that in Bob's channel.

In our experiment, only the loss in Alice's mode affects the single-photon detection rate. In the case of loss in Bob's channel, the generation rate of optical cat states is around 1 kHz, which is obtained by considering the single-photon detection rate 14 kHz and the success probability 7.5% of the post-selection procedure, and remains unchanged with the transmission efficiency η_B. In the case of loss on Alice's channel, the generation rate of optical cat states decreases with transmission efficiency η_A. The success probability of the post-selection procedure depends on the selection width, which is chosen as $\delta x = 0.05$ in our experiment. To choose a proper selection width in post-selection, the trade-off between the fidelity and the success probability should be considered (see Section S3, Supporting Information for more details).

5. Discussion and Conclusion

Up to now, it remains a challenge to prepare optical cat states with amplitude larger than 2, which is a necessary requirement for quantum computation with cat states.[11] Here, we show that our scheme can generate large-amplitude optical cat states by subtracting more photons from a TMSS with optimum squeezing. Supposing that n photons are subtracted and the homodyne projective measurement $p_A = 0$ is performed at Alice's station, Bob's state is expressed by

$$|\varphi^{(n)}_{0|\hat{p}_A}\rangle_B = N_n^{-1/2} \sum_{m=n}^{\infty} \frac{\sqrt{m!}\, i^{-(m-n)} \tanh^m r}{\sqrt{2^{m-n}}(m-n)!} H_{m-n}(0)|m\rangle_B \tag{3}$$

where N_n is the normalized parameter. When even and odd numbers of photons are subtracted, even and odd cat states are obtained, respectively. The fidelity between Bob's state and an ideal cat state is given by

$$F^{(n)}_{\pm} = \mathcal{N}'_n \left| \sum_{m=n}^{\infty} \frac{i^{-(m-n)} \tanh^m r}{\sqrt{2^{m-n}}} \frac{\alpha^m \pm (-\alpha)^m}{(m-n)!} H_{m-n}(0) \right|^2 \tag{4}$$

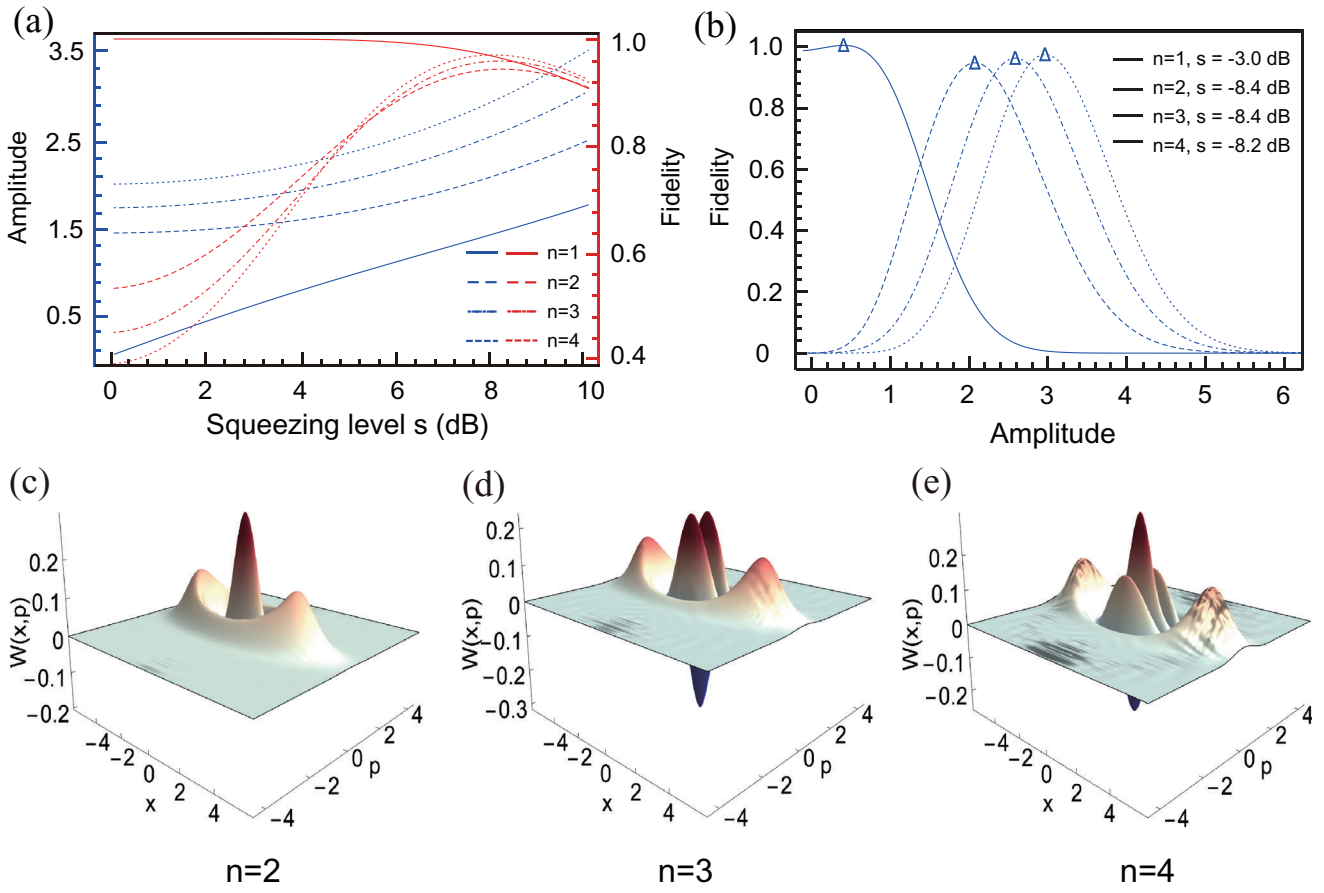

Figure 5. Results for increasing the amplitude of the prepared cat states. a) Dependence of amplitude and fidelity of Bob's cat state on the squeezing level of the TMSS for different subtracted photon numbers on Alice's mode. b) Dependence of fidelity on the amplitude of Bob's cat state with optimum squeezing levels for different subtracted photon numbers. The fidelity represents the overlap between Bob's state ρ_B and the odd cat state $|cat_-\rangle$ for odd n, and the overlap between ρ_B and the even cat state $|cat_+\rangle = (|\alpha\rangle + |-\alpha\rangle)/\sqrt{2(1+e^{-2|\alpha|^2})}$ for even n. The unit transmission efficiency is chosen in the calculation. c–e) Wigner functions of prepared cat states at Bob's station when two, three, and four photons are subtracted from Alice's mode with optimum squeezing levels of −8.4, −8.4, and −8.2 dB, respectively.

where $\mathcal{N}_n' = N_n^{-1}e^{-|\alpha|^2}/2(1 \pm e^{-2|\alpha|^2})$, and the subscripts + and − correspond to even and odd cat states, respectively.

As shown in **Figure 5**a, the amplitude of the cat state is increasing with the increase of squeezing level while the fidelity decreases slowly when one photon is subtracted by Alice (solid lines). Interestingly, by subtracting more photons, the amplitudes are increased but the fidelities reach their maximum at certain squeezing levels, which is different from the tendency of the case of single-photon subtraction. As shown in Figure 5b, it is obvious that with optimum squeezing level, the fidelity reaches the maximum for each case, the more photons are subtracted from Alice's state, the larger cat states are obtained. For example, when the squeezing level of the TMSS is 8.4 dB, by subtracting three photons, the cat state with amplitude of ≈ 2.61 and fidelity of 96% can be obtained. By comparing the Wigner functions of subtracting two, three, and four photons, as shown in Figure 5c–e respectively, the amplitude of the cat states at Bob's station is increased and the interference between two coherent components becomes more apparent. Compared with the preparation of a large-amplitude cat state by subtracting multi-photons from a squeezed vacuum state, cat states prepared by our method present higher fidelity under the same condition (see Section S1, Supporting Information for more details).

Compared with the method to prepare non-Gaussian entangled states such as N00N state and hybrid entangled state, Gaussian entangled states can be prepared deterministically and are scalable. The scalability of the Gaussian entangled state has been demonstrated with over ten thousand modes in recent years.[41,42] In a quantum network, with the increase of the number of users, it is convenient to extend our RSP scheme to multi-users based on a deterministic multipartite Gaussian entangled state.[46] It is interesting to demonstrate the RSP of optical cat states based on multipartite Gaussian entanglement, which has potential application in a quantum network and is worthy of further investigation.

In summary, we remotely prepared odd optical cat states by subtracting one photon from one mode of the TMSS and performing homodyne projective measurement on the

photon-subtracted state at Alice's station. The rotation operation is also implemented on the prepared cat states remotely by changing Alice's measurement basis of homodyne detection. We demonstrate that the remotely prepared cat state can tolerate much more loss in Alice's channel than that in Bob's channel. More importantly, we show that optical cat states with amplitudes larger than 2 can be prepared by subtracting more photons from the TMSS with optimum squeezing.

In our scheme, the techniques of photon subtraction and homodyne projective measurement are combined to realize remote preparation of optical cat state, which is a typical hybrid quantum information processing involving both discrete-variable technique and continuous-variable quantum resource. Our results present a new method to remotely prepare optical cat states and make a crucial step toward the remote hybrid quantum information processing. Inspired by the recent advance of preparing non-Gaussian quantum states by performing photon subtraction on a multimode Gaussian entangled state,[47] it would be worth to further developing our method for remotely creating cat states in a quantum network.

Supporting Information

Supporting Information is available from the Wiley Online Library or from the author.

Acknowledgements

D.H. and F.S. contributed equally to this work. This research was supported by the NSFC (Grant Nos. 11834010, 12125402, 11975026, and 12147148). X.S. acknowledges the Fund for Shanxi "1331 Project" Key Subjects Construction. Q.H. acknowledges the Beijing Natural Science Foundation (Z190005). F.S. acknowledges the China Postdoctoral Science Foundation (Grant No. 2020M680186).

Conflict of Interest

The authors declare no conflict of interest.

Data Availability Statement

The data that support the findings of this study are available from the corresponding author upon reasonable request.

Keywords

entanglement, optical cat states, photon subtraction, remote state preparation

Received: February 3, 2023
Revised: February 20, 2023
Published online: March 17, 2023

[1] H.-K. Lo, *Phys. Rev. A* **2000**, *62*, 012313.
[2] M. G. A. Paris, M. Cola, R. Bonifacio, *J. Opt. B: Quantum Semiclass. Opt.* **2003**, *5*, S360.
[3] N. Lee, H. Benichi, Y. Takeno, S. Takeda, J. Webb, E. Huntington, A. Furusawa, *Science* **2011**, *332*, 330.
[4] S. Pogorzalek, K. G. Fedorov, M. Xu, A. Parra-Rodriguez, M. Sanz, M. Fischer, E. Xie, K. Inomata, Y. Nakamura, E. Solano, A. Marx, F. Deppe, R. Gross, *Nat. Commun.* **2019**, *10*, 2604.
[5] D. W. Leung, P. W. Shor, *Phys. Rev. Lett.* **2003**, *90*, 123905.
[6] A. K. Pati, *Phys. Rev. A* **2000**, *63*, 014302.
[7] E. Schrödinger, *Naturwissenschaften* **1935**, *23*, 807.
[8] S. Haroche, *Rev. Mod. Phys.* **2013**, *85*, 1083.
[9] M. Arndt, K. Hornberger, *Nat. Phys.* **2014**, *10*, 271.
[10] H. Jeong, M. S. Kim, *Phys. Rev. A* **2002**, *65*, 042305.
[11] T. C. Ralph, A. Gilchrist, G. J. Milburn, W. J. Munro, S. Glancy, *Phys. Rev. A* **2003**, *68*, 042319.
[12] A. P. Lund, T. C. Ralph, T. C. Haselgrove, *Phys. Rev. Lett.* **2008**, *100*, 030503.
[13] A. Tipsmark, R. Dong, A. Laghaout, P. Marek, M. Ježek, U. L. Andersen, *Phys. Rev. A* **2011**, *84*, 050301(R).
[14] A. E. Ulanov, D. Sychev, A. A. Pushkina, I. A. Fedorov, A. I. Lvovsky, *Phys. Rev. Lett.* **2017**, *118*, 160501.
[15] D. V. Sychev, A. E. Ulanov, E. S. Tiunov, A. A. Pushkina, A. Kuzhamuratov, V. Novikov, A. I. Lvovsky, *Nat. Commun.* **2018**, *9*, 3672.
[16] S. J. Van Enk, O. Hirota, *Phys. Rev. A* **2001**, *64*, 022313.
[17] J. S. Neergaard-Nielsen, Y. Eto, C.-W. Lee, H. Jeong, M. Sasaki, *Nat. Photonics* **2013**, *7*, 439.
[18] M. Kira, S. W. Koch, R. P. Smith, A. E. Hunter, S. T. Cundiff, *Nat. Phys.* **2011**, *7*, 799.
[19] J. Joo, W. J. Munro, T. P. Spiller, *Phys. Rev. Lett.* **2011**, *107*, 083601.
[20] A. Gilchrist, K. Nemoto, W. J. Munro, T. C. Ralph, S. Glancy, S. L. Braunstein, G. J. Milburn, *J. Opt. B: Quantum Semiclass. Opt.* **2004**, *6*, S828.
[21] A. Ourjoumtsev, R. Tualle-Brouri, J. Laurat, P. Grangier, *Science* **2006**, *312*, 83.
[22] J. S. Neergaard-Nielsen, B. M. Nielsen, C. Hettich, K. Mølmer, E. S. Polzik, *Phys. Rev. Lett.* **2006**, *97*, 083604.
[23] K. Wakui, H. Takahashi, A. Furusawa, M. Sasaki, *Opt. Express* **2007**, *15*, 3568.
[24] H. Takahashi, K. Wakui, S. Suzuki, M. Takeoka, K. Hayasaka, A. Furusawa, M. Sasaki, *Phys. Rev. Lett.* **2008**, *101*, 233605.
[25] T. Gerrits, S. Glancy, T. S. Clement, B. Calkins, A. E. Lita, A. J. Miller, A. L. Migdall, S. W. Nam, R. P. Mirin, E. Knill, *Phys. Rev. A* **2010**, *82*, 031802(R).
[26] D. V. Sychev, A. E. Ulanov, A. A. Pushkina, M. W. Richards, I. A. Fedorov, A. I. Lvovsky, *Nat. Photonics* **2017**, *11*, 379.
[27] M. Zhang, H. Kang, M. Wang, F. Xu, X. Su, K. Peng, *Photon. Res.* **2021**, *9*, 887.
[28] U. L. Andersen, J. S. Neergaard-Nielsen, P. V. Loock, A. Furusawa, *Nat. Phys.* **2015**, *11*, 713.
[29] M. Walschaers, N. Treps, *Phys. Rev. Lett.* **2020**, *124*, 150501.
[30] Y. Xiang, S. Liu, J. Guo, Q. Gong, N. Treps, Q. He, M. Walschaers, *npj Quantum Inf.* **2022**, *8*, 21.
[31] S. Liu, D. Han, N. Wang, Y. Xiang, F. Sun, M. Wang, Z. Qin, Q. Gong, X. Su, Q. He, *Phys. Rev. Lett.* **2022**, *128*, 200401.
[32] A. Ourjoumtsev, H. Jeong, R. Tualle-Brouri, P. Grangier, *Nature* **2007**, *448*, 784.
[33] A. E. Ulanov, I. A. Fedorov, D. Sychev, P. Grangier, A. I. Lvovsky, *Nat. Commun.* **2016**, *7*, 11925.
[34] H. L. Jeannic, A. Cavailles, J. Raskop, K. Huang, J. Laurat, *Optica* **2018**, *5*, 001012.
[35] B. Hacker, S. Welte, S. Daiss, A. Shaukat, S. Ritter, L. Li, G. Rempe, *Nat. Photonics* **2019**, *13*, 110.
[36] F.-X. Sun, S.-S. Zheng, Y. Xiao, Q. Gong, Q. He, K. Xia, *Phys. Rev. Lett.* **2021**, *127*, 087203.
[37] C. Weedbrook, S. Pirandola, R. García–Patrón, N. J. Cerf, T. C. Ralph, J. H. Shapiro, S. Lloyd, *Rev. Mod. Phys.* **2012**, *84*, 621.

[38] S. Yokoyama, R. Ukai, S. C. Armstrong, C. Sornphiphatphong, T. Kaji, S. Suzuki, J.-I. Yoshikawa, H. Yonezawa, N. C. Menicucci, A. Furusawa, *Nat. Photonics* **2013**, *7*, 982.
[39] J. Roslund, R. M. de Araújo, S. Jiang, C. Fabre, N. Treps, *Nat. Photonics* **2014**, *8*, 109.
[40] M. Chen, N. C. Menicucci, O. Pfister, *Phys. Rev. Lett.* **2014**, *112*, 120505.
[41] W. Asavanant, Y. Shiozawa, S. Yokoyama, B. Charoensombutamon, H. Emura, R. N. Alexander, S. Takeda, J.-I. Yoshikawa, N. C. Menicucci, H. Yonezawa, A. Furusawa, *Science* **2019**, *366*, 369.
[42] M. V. Larsen, X. Guo, C. R. Breum, J. S. Neergaard-Nielsen, U. L. Andersen, *Science* **2019**, *366*, 373.
[43] Y. Liu, Z. Ma, H. Kang, D. Han, M. Wang, Z. Qin, X. Su, K. Peng, *npj Quantum Inf.* **2019**, *5*, 68.
[44] X. Dfeng, Y. Liu, M. Wang, X. Su, K. Peng, *npj Quantum Inf.* **2021**, *7*, 65.
[45] M. Wang, Y. Xiang, H. Kang, D. Han, Y. Liu, Q. He, Q. Gong, X. Su, K. Peng, *Phys. Rev. Lett.* **2020**, *125*, 260506.
[46] D. Han, N. Wang, M. Wang, Z. Qin, X. Su, *Opt. Lett.* **2022**, *47*, 3295.
[47] Y.-S. Ra, A. Dufour, M. Walschaers, C. Jacquard, T. Michel, C. Fabre, N. Treps, *Nat. Phys.* **2020**, *16*, 144.